Supporting Information for
Allosteric modulation of Grb2 recruitment to the intrinsically disordered scaffold protein, LAT, by remote site phosphorylation

William Y. C. Huang[1,2,‡], Jonathon A. Ditlev[1,3,‡], Han-Kuei Chiang[2], Michael K. Rosen[1,3,*], Jay T. Groves[1,2,*]

[1] The Howard Hughes Medical Institute Summer Institute, Marine Biological Laboratory, Woods Hole, MA, 02543, United States
[2] Department of Chemistry, University of California, Berkeley, Berkeley, CA 94720, United States
[3] Department of Biophysics and Howard Hughes Medical Institute, University of Texas Southwestern Medical Center, Dallas, TX, 75390

[*]To whom correspondence should be addressed: michael.rosen@utsouthwestern.edu jtgroves@lbl.gov.

[‡]These authors contributed equally to this work.

SI Text

An Empirical Model for LAT Allostery

The nonlinear dependence of LAT:Grb2 binding affinity can be considered by the pair-wise additions of multivalent allosteric interactions (Fig. S4A):

$$K^{(4Y)} = \sum_{i=1}^{f} K_i^{(1Y)} \left(\sum_{j=1}^{f} \varepsilon_{ji}(f) \right) \quad \text{Eq. [S1]}$$

where K is the binding affinity with a subscript denoting the tyrosine site (i.e. 1 to 4 in the case of LAT used in the experiments), $\varepsilon_{ji}(f)$ denotes the effective allosteric interaction from site *j* to site *i* and $\varepsilon_{ji} = 1$ when $i = j$, f is the multivalency. Note that the specific type of allosteric interactions is not assumed in the model, $\varepsilon_{ji}(f)$ can be a result of conformational changes or other form of structural communication. The binding kinetics for different constructs of LAT are reflected in the $\varepsilon_{ji}(f)$ terms, e.g. $K_{FYYY}^{(3Y)} = K_{FYFF}^{(1Y)}(1 + \varepsilon_{32} + \varepsilon_{42}) + K_{FFYF}^{(1Y)}(\varepsilon_{23} + 1 + \varepsilon_{43}) + K_{FFFY}^{(1Y)}(\varepsilon_{24} + \varepsilon_{34} + 1)$. Further analysis can be made by considering different form of $\varepsilon_{ji}(f)$.

The allosteric interactions depend solely on pair-wise residues involved

In the simplest mean field treatment of the allosteric interactions:

$$\varepsilon_{ji}(f) = \begin{cases} \varepsilon, & both\ the\ i\ and\ j\ sites\ are\ present \\ 0, & otherwise \end{cases}$$

Eq. [S1] can be rearranged into $\langle K^{(fY)} \rangle = f(1 + (f-1)\varepsilon)\langle K_i^{(1Y)} \rangle$. This simple assumption predicts that $\langle K^{(fY)} \rangle \propto f^2$. Fitting of this curve to the experiments yields $\varepsilon = 0.98$ (Fig. S4B).

The allosteric interactions depend on the total multivlency

Since empirical fitting of the above data to a power law yields an order of ~3, it remains possible that the $\varepsilon_{ji}(f)$ terms depends on the total multivalency, i.e. there are synergies in the binding affinity between each and every site:

$$\varepsilon_{ji}(f) = \begin{cases} \varepsilon(f), & both\ the\ i\ and\ j\ sites\ are\ present \\ 0, & otherwise \end{cases}$$

Eq. [1] is rearranged into $\langle K^{(fY)} \rangle = (f + f(f-1)\varepsilon(f))\langle K_i^{(1Y)} \rangle$. Taken with the empirical fits, this analysis predicts that $\varepsilon(f) \propto f$. Fitting the data with $K^{(fY)} = (f + f(f-1)\alpha f)K_i^{(1Y)}$ gives $\alpha = 0.26$ (Fig. S4C).

SI Methods and Materials

Methods and materials used in this study were similar to previous studies [1,2].

Chemicals

1,2-dioleoyl-sn-glycero-3-phosphocholine (DOPC) and 1,2-dioleoyl-sn-glycero-3-[(N-(5-amino-1-carboxypentyl)iminodiacetic acid)succinyl] (nickel salt) (Ni^{2+}-NTA-DOGS) were purchased from Avanti Polar Lipids. Texas Red 1,2-dihexadecanoylsn-glycero-3-phosphoethanolamine (TR-DHPE) was purchased from Invitrogen. Alexa Fluor 647 maleimide dye and Alexa Fluor 561 maleimide dye were purchased from Life Technology. Bovine Serum Albumin (BSA), (±)-6-Hydroxy-2,5,7,8-tetramethylchromane-2-carboxylic acid (Trolox), Catalase, 2-Mercaptoethanol (BME), $NiCl_2$, H_2SO_4 and ATP were purchased from Sigma-Aldrich. Glucose Oxidase was purchased from Serva. Tris(2-carboxyethyl)phosphine (TCEP) was brought from Thermo Scientific. Glucose and H_2O_2 were from Fisher Scientific. $MgCl_2$ was from EMD Chemicals. Tris buffer saline (TBS) was purchased from Corning.

Protein Purification

TCR ζ chain

BL21(DE3) cells containing human CD3ζ (residues 52-164) fused with an N-terminal His_{10} tag were collected by centrifugation and lysed by cell disruption (Emulsiflex-C5, Avestin) in 20 mM HEPES (pH 7.5), 5 mM imidazole (pH 7.0), 150 mM NaCl, 1 mM $MgCl_2$, 5% glycerol, 5 mM βME, 1 mM PMSF, 1 μg/ml antipain, 1 μg/ml pepstatin, and 1 μg/ml leupeptin. Centrifuge-cleared lysate was applied to Ni-NTA Agarose (Qiagen), washed three times with 25 mM HEPES (pH 7.5), 30 mM imidazole (pH 7.0), 300 mM NaCl, and 5 mM βME and eluted step-wise with 25 mM HEPES (pH 7.5), 100 mM imidazole (pH 7.0), 300 mM NaCl, and 5 mM βME followed by elution with 25 mM HEPES (pH 7.5), 500 mM imidazole (pH 7.0), 300 mM NaCl, and 5 mM βME. Protein was applied to a Superdex 200 prepgrade column (GE Healthcare) in 25 mM HEPES (pH 7.5), 300 mM NaCl, 1 mM $MgCl_2$, and 2 mM βME. CD3ζ was concentrated using Amicon Ultra 3K Centrifugal Filter units (Millipore) to > 150 μM, mixed with 100 mM HEPES (pH 7.5), 300 mM NaCl, 15 mM ATP, 20 mM $MgCl_2$, 1 mM DTT, and 400 nM Lck and incubated for 16 hr at 30°C. Phosphorylated protein was applied to a Superdex 75 GL column (GE Healthcare) in 25 mM HEPES (pH 7.5), 300 mM NaCl, 1 mM $MgCl_2$, and 2 mM βME. 100% phosphorylation was confirmed by mass spectrometry.

Grb2

Coding sequences for full-length Grb2 were amplified by PCR and cloned into a pET-28-derived bacterial expression vector by use of NdeI and XhoI sites. A tobacco etch virus (TEV) protease cleavage site was engineered between the N-terminal 6-His tag and the NdeI site. Grb2 constructs was then transformed into the BL21 strain of *E. coli*. The expression of recombinant Grb2 was induced by adding 0.2 mM IPTG for 16 h at 18°C. The bacterial cells were then resuspended in lysis buffer containing 20 mM Tris-HCl, 150 mM NaCl, 25 mM imidazole, and 5 mM BME at pH 8.0, lysed using a French press and centrifuge to remove cellular debris at 17,000 rpm for 1 h at 4°C. The clarified lysate was passed through a Ni-nitrilotriacetic acid (Ni-NTA) column (Qiagen). The recombinant protein was eluted from the column by using a buffer containing 20 mM Tris-HCl, 150 mM NaCl, 250 mM imidazole, and 5 mM BME at pH 8.0. The eluted Grb2 was incubated overnight with TEV protease to remove the N-terminal His tag. The protein was concentrated by ultrafiltration and further purified by size exclusion chromatography (Superdex 200). The final buffer for the gel filtration step was 20 mM Tris-HCl, 150 mM NaCl, 5 mM TCEP, and 100 mM arginine at pH 7.5.

LAT (all variants)

BL21(DE3) cells containing MBP-His_8-LAT 48-233-His_6 were collected by centrifugation and lysed by cell disruption (Emulsiflex-C5, Avestin) in 20 mM imidazole (pH 8.0), 150 mM NaCl, 5 mM βME, 0.1% NP-40, 10% glycerol, 1 mM PMSF, 1 μg/ml antipain, 1 μg/ml pepstatin, and 1 μg/ml leupeptin. Centrifugation-cleared lysate was applied to Ni-NTA agarose (Qiagen), washed with 10 mM imidazole (pH 8.0), 150 mM NaCl, 5 mM βME, 0.01% NP-40, and 10% glycerol, and eluted with 500 mM imidazole (pH 8.0), 150 mM NaCl, 5 mM βME, 0.01% NP-40, and 10% glycerol. MBP and His_6 tag were removed using

TEV protease treatment for 16 hrs at 4°C. Cleaved protein was applied to a Source 15 Q anion exchange column and eluted with a gradient of 200 mM→300 mM NaCl in 20 mM HEPES (pH 7.0) and 2 mM DTT followed by size exclusion chromatography using a Superdex 200 prepgrade column (GE Healthcare) in 25 mM HEPES (pH 7.5), 150 mM NaCl, 1 mM $MgCl_2$, and 1 mM DTT. To phosphorylate LAT variants prior to membrane binding, purified LAT was concentrated using Amicon Ultra 3K Centrifugal Filter units (Millipore) to >400 μM, mixed with 25 mM HEPES (pH 7.5), 150 mM NaCl, 15 mM ATP, 20 mM $MgCl_2$, 2 mM DTT and 2.4 μM ZAP-70, and incubated for 24 hrs at 30°C. Phosphorylated LAT was applied to a Mono Q anion exchange column and eluted using a shallow 250 mM → 320 mM NaCl over 70 column volumes gradient in 25 mM HEPES (pH 7.5), 1 mM $MgCl_2$, and 2 mM βME to resolve differentially phosphorylated species of LAT. YYYY, FYYY, YFYY, YYFY, YYYF, YFFF, FYFF, FFYF, and FFFY LAT phosphorylation was confirmed by mass spectrometry.

Lck

Human Lck kinase fused to a His_6 tag was expressed in SF9 cells using the Bac-to-Bac baculovirus expression system (Life Technologies). The infected cells were harvested in 50 mM Tris (pH 7.5), 100 mM NaCl, 5 mM βME and 0.01% NP-40, 1 mM PMSF, 1 μg/ml antipain, 1 mM benzamidine, and 1 μg/ml leupeptin. Cells were lysed using a cell disruptor (Emulsiflex-C5, Avestin) in 50 mM Tris (pH 7.5), 100 mM NaCl, 5 mM βME and 0.01% NP-40, 1 mM PMSF, 1 μg/ml antipain, 1 mM benzamidine, and 1 μg/ml leupeptin. The cleared lysate was applied to Ni-NTA agarose beads equilibrated with 20 mM Tris pH (7.5), 500 mM NaCl, 20 mM imidazole, 5 mM βME, and 10% glycerol, washed with 20 mM Tris (pH 7.5), 1 M NaCl, 5 mM βME and 0.01% NP-40, and then eluted with 20 mM Tris (pH 7.5), 200 mM imidazole 7.5 and 100 mM NaCl. The elute was applied to a Source 15 Q column using a gradient of 100 → 300 mM NaCl in 25 mM HEPES (pH 7.5) and 2 mM βME. Collected fractions were concentrated Amicon Ultra 10K Centrifugal Filter units and applied to an Superdex75 prepgrade (GE Healthcare) size exclusion column in 25 mM HEPES (pH 7.5), 150 mM NaCl, and 1 mM βME.

ZAP-70

Human ZAP70 with an N terminal SNAP-tag was expressed as a GST fusion protein in SF9 cells using the Bac-to-Bac baculovirus expression system (Life Technologies), with a PreScission recognition sequence (LEVLFQGP) engineered between the GST and SNAP-tag. The infected cells were lysed using a cell disruptor (Emulsiflex-C5, Avestin) in 50 mM HEPES (pH 7.5), 200 mM NaCl, 5 mM βME, 1 mM PMSF, 1 μg/ml antipain, 1 μg/ml pepstatin, and 1 μg/ml leupeptin. Centrifugation-cleared lysate was applied to Glutathione Sepharose 4B (GE Healthcare) and washed three times with 50 mM HEPES (pH 7.5), 200 mM NaCl, and 5 mM βME. Protein was then cleaved on-column with HRV3C protease (Novagen) treatment for 16 hrs at 4°C to remove the GST tag and eluted. Cleaved protein was applied to a Superdex 200 prepgrade (GE Healthcare) size exclusion column in 50 mM HEPES (pH 7.5), 300 mM NaCl, and 2 mM βME. Purified ZAP-70 was concentrated using Amicon Ultra 30K Centrifugal Filter units to > 50 μM. SNAP Surface-Alexa Fluor 488 (New England Biolabs) was added to ZAP-70 at 85 μM and incubated at room temperature for 1 hr. Labeled protein was applied to a Superdex 200 GL (GE Healthcare) size exclusion column in 50 mM HEPES (pH 7.5), 300 mM NaCl, and 2 mM βME.

Protein labeling using maleimide

LAT and Grb2 were diluted to 100 μM (or less). Grb2 was then allowed to react with 1 mM C_5-maleimide Alexa Fluor 568 or C_2-maleimide Alexa Fluor 647 for 2 hrs at room temperature. The reaction was then quenched with 5 mM BME for 10 min. Excess dye was removed by size exclusion chromatography using a Sephadex G-25 column. C_5-maleimide Alexa Fluor488 (or Alexa Fluor 568) was added in excess to pLAT in reducing agent-free buffer and incubated for 16 hrs at 4°C. Following the incubation 5 mM βME was added to the labeling solution to quench the reaction. Excess dye was removed from Alexa488-labeled pLAT by size exclusion chromatography in 25 mM HEPES (pH 7.5), 150 NaCl, 1 mM $MgCl_2$, 1 mM βME, and 10% glycerol using a Superdex 75 column.

Isothermal Titration Calorimetry

Grb2 and LAT 1Y variants were dialyzed in the same buffer [20 mM HEPES (pH 7.5), 136 mM NaCl, 5 mM $MgCl_2$, and 1 mM TCEP] overnight before using them for isothermal calorimetry measurements. Measurements were performed at 15 °C on an MicroCal iTC_{200} instrument from Malvern. Isotherms were analyzed using the software NITPIC [3], and fits were performed using the software SEDPHAT [4].

Functionalized Supported Membranes

Glass substrates (no. 1.5 thickness) were prepared by 5 min piranha etching (H_2SO_4:H_2O_2 = 3:1 by volume), followed by excessive rinsing of H_2O (Milli-Q). Glass substrates were blow dried with air before depositing small unilamellar vesicles (SUVs) to form supported lipid bilayers (SLBs). SUVs were prepared by mixing DOPC: Ni^{2+}-NTA-DOGS = 96:4 by molar percent in chloroform. If visualization of the bilayers was required, additional 0.005% of TR-DHPE was added to the lipid composition. The solution mixture was then evaporated using a rotary evaporator for 15 min at 40°C. Dried lipid films were further dried with N_2 for 15 min. Lipids were resuspended in H_2O by vortexing, resulting in a concentration of ~0.5 mg/mL. Finally, the vesicle solution was sonicated for 90 s in an ice-water bath. The membrane system was prepared on a flow chamber (μ-Slide, Ibidi). SLBs were formed on a glass substrate by incubating the SUVs mixed with 40 mM TBS for at least 30 min. The chambers were rinsed with TBS buffer and incubated with 100 mM $NiCl_2$ for 5 min. TBS buffer refers to 20 mM TBS buffer with 5mM $MgCl_2$ at pH 7.4 unless stated otherwise. Next, 1 mg/mL BSA in TBS buffer was incubated for 10 min to block defects in supported membranes. Before protein incubation, the system was buffer exchanged into TBS buffer containing 1 mM TCEP. Proteins were centrifuged for 20 min at 4°C beforehand to remove possible aggregates. Depending on the desired density of the membrane proteins, LAT (or other mutants of LAT) and TCRζ chain were incubated between 10-500 nM for 10 min to attach to the bilayers via his-tag – Ni^{2+}NTA chemistry [5]. The system was allowed to sit for another 20 min to allow unstably bound membrane proteins to dissociate from the surface. Between all incubation steps, the chambers were rinsed with TBS buffer. Fluidity of the membrane-bound proteins was examined by fluorescent recovery after photobleaching (FRAP). Densities of membrane proteins were estimated by establishing a calibration curve between epifluorescence average intensity and densities measured by fluorescence correlation spectroscopy (FCS) (FCS methods were described previously [6]). Phosphorylation of LAT was triggered by injection of 500 pM ZAP-70, 50 nM Grb2 and 1 mM ATP in scavenger buffer (2 mM UV-treated trolox, 10 mM BME, 20 mM glucose, 320 μg/mL glucose oxidase, 50μg/mL catalase [7]). Prior to the injection, ZAP-70 was incubated with 1 mM ATP for 30 min. All parts of preparation were done at room temperature unless otherwise stated.

Microscopy

TIRF experiments were performed on a motorized inverted microscope (Nikon Eclipse Ti-E; Technical Instruments, Burlingame, CA) equipped with a motorized Epi/TIRF illuminator, motorized Intensilight mercury lamp (Nikon C-HGFIE), Perfect Focus system, and a motorized stage (Applied Scientific Instrumentation MS-2000, Eugene, OR). A laser launch with 488 and 640 nm (Coherent OBIS, Santa Clara, CA) diode lasers was controlled by an OBIS Scientific Remote (Coherent Inc., Santa Clara, CA) and aligned into a fiber launch custom built by Solamere Technology Group, Inc. (Salt Lake City, UT). The optical path was then aligned to a 100x 1.49 NA oil immersion TIRF objective (Nikon). A dichroic beamsplitter (z488/647rpc; Chroma Technology Corp., Bellows Falls, VT) reflected the laser light through the objective lens and fluorescence images were recorded using an EM-CCD (iXon 897DU; Andor Inc., South Windsor, CT) after passing through a laser-blocking filter (Z488/647M; Chroma Technology Corp., Bellows Falls, VT). Laser powers measured at the sample were 10 mW and 0.6 mW for 488 nm and 647 nm, respectively. Exposure times were set to 40 ms and 20 ms for 488 nm and 647 nm, respectively. All acquisitions were obtained using Micro-Manager [8]. A TTL signal from the appropriate laser triggered the camera exposure.

Imaging of ZAP-70 and Grb2

All imaging experiments were performed in imaging buffer consisted of 2 mM UV-treated trolox, 10 mM βME, 20 mM glucose, 320 μg/mL glucose oxidase, 50 μg/mL catalase [7] and 0.1 mg/mL BSA in TBS buffer. For the experiments in Fig. 1, 2 and 4, a set of acquisition included imaging Grb2 then ZAP-70 with less than 500 ms between them. The time interval between each set of acquisition was 2 s, minimizing

photobleaching while allowing Grb2 to dynamically sample the pY density. Analysis was performed on the central circle with a diameter of 200 pixel region of the images to minimize uneven illumination. The intensities were then background-subtracted and convert to densities of molecules using calibration curve from FCS. Initial rate analysis was performed at early timepoint of the phosphorylation (Fig. 3A) where the rates were approximately constant using Eq. [1] (Fig. 4). All epifluorescence images were analyzed with Fiji and Igor.

Self-consistency analysis

To compare rates of LAT4Y phosphorylation from LAT1Y or LAT4Y data (Fig. 4), the Grb2 intensities LAT4Y data were first transformed into corresponding pY densities using the empirical nonlinear binding kinetics (Fig. 2D). During this transformation, the degree of phosphorylation (λ) needed to be assumed to account for the allosteric effect, i.e. processive phosphorylation corresponded to more Grb2 recruited when compared to distributive phosphorylation of the same pY production. Therefore, $v_{LAT4Y}(\lambda) = \frac{Intensity\ of\ Grb2}{(Ratio\ of\ Grb2\ intensity\ to\ LAT4Y\ density)\times K(\lambda)} \times \lambda$, where $K(\lambda)$ is the relative binding kinetics. This assumption can be compared with the expected rates of LAT4Y phosphorylation by LAT1Y. This was done by calculating the averaged phosphorylation rate of LAT1Y weighted by the degree of processivity (the assumption), i.e. strongly processive phosphorylation should result in a 4-fold increase in phosphorylation rate when compared to distributive mechanism given the same pY production. If the assumption is valid, the expected rate from LAT1Y should be equal to the corrected data from LAT4Y. This argument is summarized in Eq. [2].

Dwell time analysis

Single-molecule data were analyzed with customized program written in Igor [1] (Fig. 3). Analysis was performed on the central 350x350 pixel region of the images to minimize uneven illumination. The dwell time of each binding event was sorted into a histogram with the frame interval as the bin. The histogram was normalized and fitted to a probability distribution of multi-exponential kinetics:

$$p(t) = \sum_{i=1}^{N} \alpha_i k_i e^{-k_i t} \qquad \text{Eq. [S2]}$$

where N was the number of population, α_i was the fraction of the population i and k_i was the rate constant for the population i. A typical histogram consisted of 2,000-5,000 data points. Fitting procedure initiated with a single exponential. In cases of poor fitting, a maximum of two populations was used.

For single-molecule imaging of Grb2, LAT was fully phosphorylated before acquisition. Bleaching of the dye was estimated using immobilized proteins deposited on glass substrates under identical optical conditions. The Grb2 dwell time histogram requires at least two populations for a proper fit. Given that the dwell time histogram of immobilized Grb2 (bleaching curve) also exhibit a bi-exponential kinetics, the two populations most likely correspond to the photophysics of the dye. To estimate the actual off rates of pY:Grb2, we use the relation, $k_{app} = k_{-1} + k_{bl}$ [1], on the population characterized by slower kinetics (the fast kinetics are on the order of the camera rate).

Input-response function of LAT signaling

The input-response function of LAT (Fig. 5) is calculated based on the empirical characterization of the binding kinetics between LAT:Grb2 (Fig. 2D). To account of the randomness of phosphorylation, the probability of each number of phosphorylation (n) is estimated by a truncated Poisson distribution, $p(n \le f; \lambda) = \frac{\lambda^k}{k!} e^{-\lambda}/N$, where $N = 1 - \sum_{i>f} \frac{\lambda^i}{i!} e^{-\lambda}$, f is the degree of multivalency (= 4 for LAT), λ is the mean of the original Poisson distribution. The input-response function is then: $R = \sum_{i=0}^{f} p(i \le f; \lambda) \langle K^{(iY)} \rangle$ where $\langle K^{(iY)} \rangle$ is the empirically quantified binding kinetics (Fig. 2D); the corresponding mean number of phosphotyrosine (i.e. the true mean here) $= \sum_{i=0}^{f} p(i \le f; \lambda) * i$. In these calculations, we did

not consider randomness of processivity for simplicity (it is most likely a small effect for a purely distributive or strongly processive mechanism). In the case of weakly processive mechanism, we assume that the phosphorylation of LAT happens from none to two to four phosphotyrosine. The sensitivity is the first derivative of the input-response function, $\frac{dR}{dpY}$.

SI Reference

(1) Huang, W. Y. C.; Yan, Q.; Lin, W. C.; Chung, J.; Hansen, S. D.; Christensen, S. M.; Tu, H. L.; Kuriyan, J.; Groves, J. T. *Proc. Natl. Acad. Sci. USA* **2016**, *113*, 8218-8223.

(2) Su, X.; Ditlev, J. A.; Hui, E. F.; Xing, W. M.; Banjade, S.; Okrut, J.; King, D. S.; Taunton, J.; Rosen, M. K.; Vale, R. D. *Science* **2016**, *352*, 595-599.

(3) Keller, S.; Vargas, C.; Zhao, H. Y.; Piszczek, G.; Brautigam, C. A.; Schuck, P. *Analytical Chemistry* **2012**, *84*, 5066-5073.

(4) Houtman, J. C. D.; Brown, P. H.; Bowden, B.; Yamaguchi, H.; Appella, E.; Samelson, L. E.; Schuck, P. *Protein Sci.* **2007**, *16*, 30-42.

(5) Nye, J. A.; Groves, J. T. *Langmuir* **2008**, *24*, 4145-4149.

(6) Lin, W. C.; Iversen, L.; Tu, H. L.; Rhodes, C.; Christensen, S. M.; Iwig, J. S.; Hansen, S. D.; Huang, W. Y. C.; Groves, J. T. *Proc. Natl. Acad. Sci. USA* **2014**, *111*, 2996-3001.

(7) Cordes, T.; Vogelsang, J.; Tinnefeld, P. *J. Am. Chem. Soc.* **2009**, *131*, 5018-5019.

(8) Edelstein AD, T. M., Amodaj N, Pinkard H, Vale RD, Stuurman N. *J Biol Methods* **2014**, *1*, e10.

SI Figures and Tables

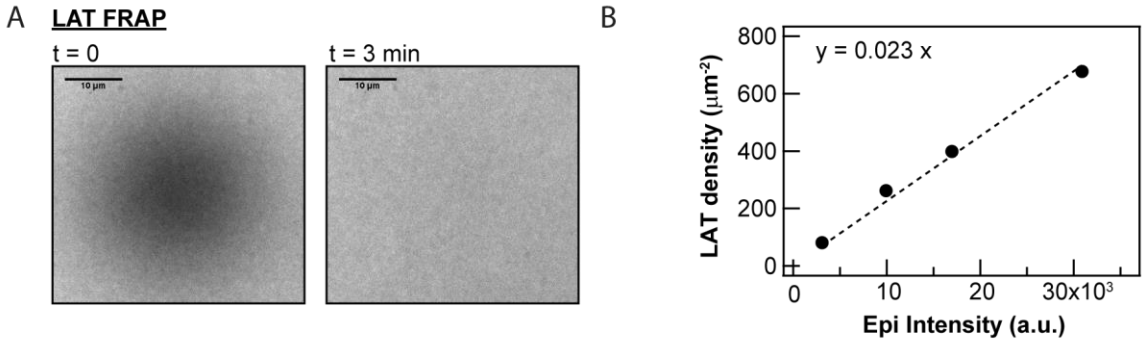

Figure S1. Characterization of LAT on supported membranes
(A) Fluorescent recovery after photobleaching (FRAP) of LAT-Alexa Fluor 568 on supported membranes. In all the reconstitution experiments, LAT has a mobile fraction of > 90%, as determined by the recovery fraction after 3 min of initial bleaching. (B) A calibration curve between epifluorescence intensity and LAT densities measured by FCS.

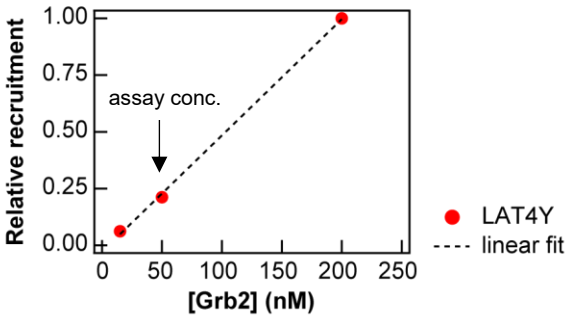

Figure S2. Binding curve of pY:Grb2

Grb2 recruitment as a function of Grb2 concentration. Grb2 recruitment is well described by a linear fit, suggesting that Grb2 is not saturating pY on membranes for all tested concentrations. Solution ITC measures pY:Grb2 interactions have K_D of 100-1000 nM (Table 1). Since our assay uses 50 nM Grb2 as a molecular sensor to probe LAT phosphorylation, each LAT will have, on average, less than one Grb2 bound to it. An additional benefit of using Grb2 at this concentration is that Grb2 in solution contributes very little fluorescent signal.

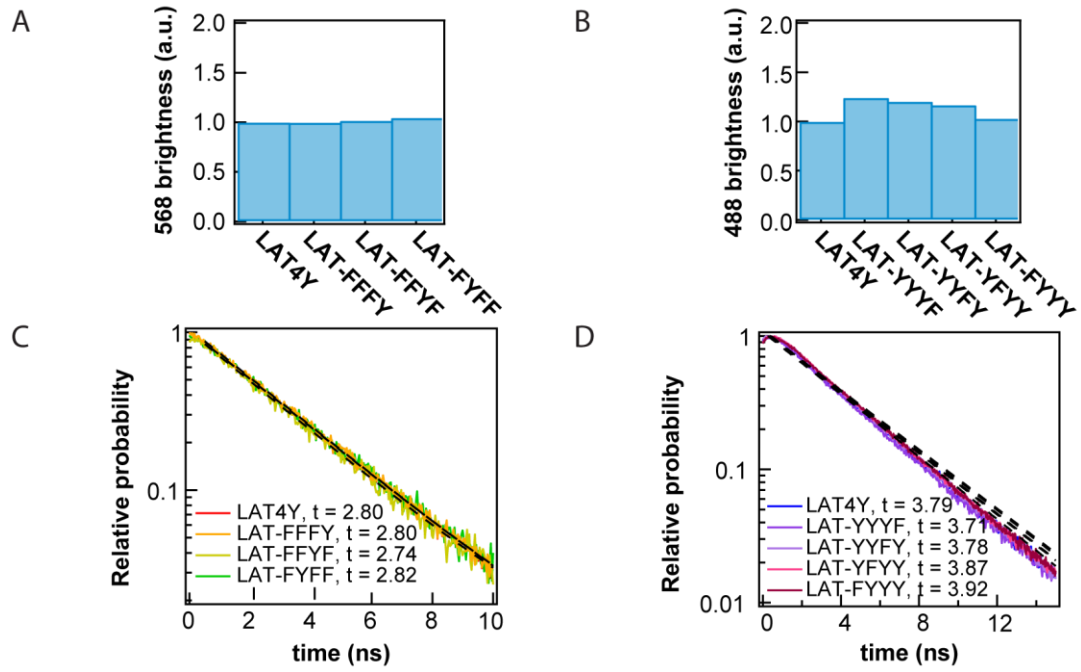

Figure S3. Photophysics of LAT-Alexa Fluor 568 or LAT-Alexa Fluor 488
(A)(B) Brightness analysis (number of photons per molecule per second) from FCS. (C)(D) Lifetime analysis from TCSPC measurements. LAT1Y and LAT3Y are labeled with Alexa Fluor 568 and Alexa Fluor 488, respectively. LAT4Y are labeled with either Alexa Fluor 568 or Alexa Fluor 488. These analyses show that photophysics across different LAT constructs is very similar.

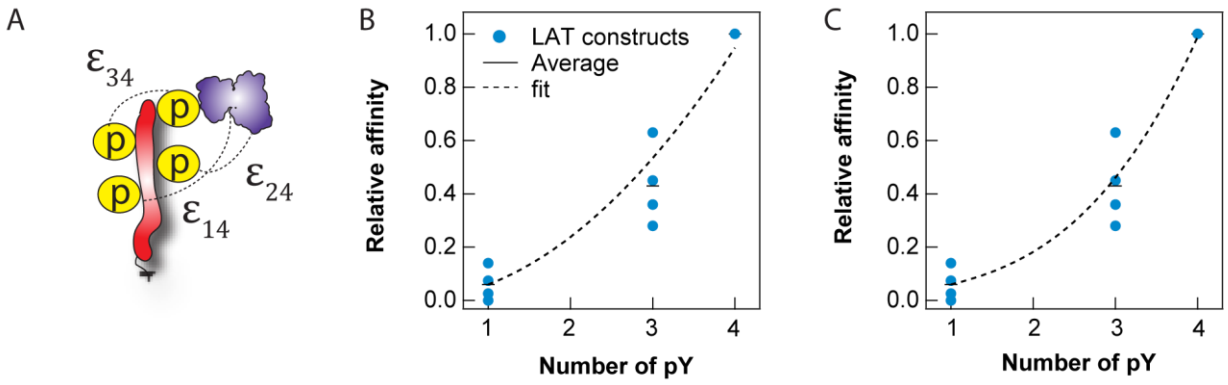

Figure S4. A model for LAT allostery
(A) A simple model for LAT allostery based on effective pair-wise interactions (ε_{ji}) between the pY residues. (B) Fitting based on a constant pair-wise interaction. (C) Fitting based on pair-wise interactions that depend on the total number of pY per LAT.

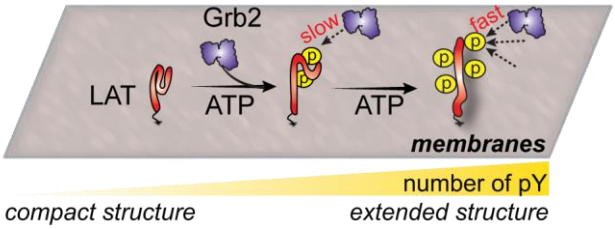

Figure S5. Molecular mechanism of LAT allostery

Increase in the number of pY increase the magnitude of the net charge of LAT, therefore extending the structure rendering the pY sites more accessible for Grb2 binding.

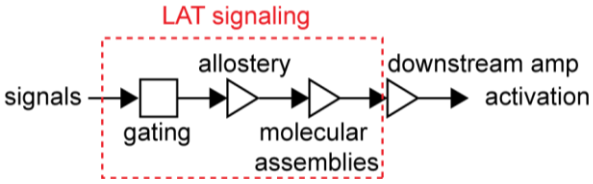

Figure S6. An operational model of signaling through LAT
Signaling through LAT are gated for low density of pY. For substantial production of pY, two mechanisms of signal amplification takes place: the recruitment of Grb2 is enhanced by the allosteric mechanism (increased on-rate) and by molecular assembly of LAT:Grb2:SOS (longer dwell-times).

Number of pY	LAT construct	abbreviation
4 (LAT4Y)	LAT	LAT4Y
3 (LAT3Y)	LAT-Y226F	LAT-YYYF
	LAT- Y191F	LAT-YYFY
	LAT- Y171F	LAT-YFYY
	LAT-Y132F	LAT-FYYY
1 (LAT1Y)	LAT-Y132F-Y171F-Y191F	LAT-FFFY
	LAT-Y132F-Y171F-Y226F	LAT-FFYF
	LAT-Y132F-Y191F-Y226F	LAT-FYFF
	LAT-Y171F-Y191F-Y226F	LAT-YFFF

Table S1. LAT abbreviations

All LAT constructs have all other Y mutated to F.

Construct	Sequence	Notes
CD3ζ	MGSSHHHHHHHHHHSSGLVPRGSHMASMTGG QQMGRGSKKCKGSRVKFSRSADAPAYQQGQN QLYNELNLGRREEYDVLDKRRGRDPEMGGKP QRRKNPQEGLYNELQKDKMAEAYSEIGMKGE RRRGKGHDGLYQGLSTATKDTYDALHMQALP PR	Human cytoplasmic fragment, residues 52 - 164 , fused with an N-terminal His_{10} tag
Grb2	GPLGSMEAIAKYDFKATADDELSFKRGDILKVL NEECDQNWYKAELNGKDGFIPKNYIEMKPHP WFFGKIPRAKAEEMLSKQRHDGAFLIRESESAP GDFSLSVKFGNDVQHFKVLRDGAGKYFLWVV KFNSLNELVDYHRSTSVSRNQQIFLRDIEQVPQ QPTYVQALFDFDPQEDGELGFRRGDFIHVMDN SDPNWWKGACHGQTGMFPRNYVTPVNRNV	Human, residues 1 - 217.
LAT	GGSLEHHHHHHHHGIQFKRPHTVAPWPPAFPP VTSFPPLSQPDLLPIPRSPQPLGGSHRTPSSRRDS DGANSVASFENEEPACEDADEDEDDFHNPGYL VVLPDSTPATSTAAPSAPALSTPGIRDSAFSMESI DDYVNVPESGESAEASLDGSREYVNVSQELHP GAAKTEPAALSSQEAEEVEEEGAPDYENLQEL N	Human, residues 48-233 (short isoform) with His_8 N-terminal fusion. This construct only contains the four C-terminal Y residues (Y132, Y171, Y191, and Y226) that are sufficient for TCR signaling. Y171, Y191, and Y226 (in red) are the three Y that are recognized by Grb2 when phosphorylated. All other Y were mutated to F.
LAT-YFFF	GGSLEHHHHHHHHGIQFKRPHTVAPWPPAFPP VTSFPPLSQPDLLPIPRSPQPLGGSHRTPSSRRDS DGANSVASFENEEPACEDADEDEDDFHNPGYL VVLPDSTPATSTAAPSAPALSTPGIRDSAFSMESI DDFVNVPESGESAEASLDGSREFVNVSQELHPG AAKTEPAALSSQEAEEVEEEGAPDFENLQELN	Human, residues 48-233 (short isoform) with His_8 N-terminal fusion. This construct only contains one C-terminal Y residue (Y132). All other Y, including Y171, Y191, and Y226, were mutated to F.
LAT-FYFF	GGSLEHHHHHHHHGIQFKRPHTVAPWPPAFPP VTSFPPLSQPDLLPIPRSPQPLGGSHRTPSSRRDS DGANSVASFENEEPACEDADEDEDDFHNPGFL VVLPDSTPATSTAAPSAPALSTPGIRDSAFSMESI DDYVNVPESGESAEASLDGSREFVNVSQELHP GAAKTEPAALSSQEAEEVEEEGAPDFENLQELN	Human, residues 48-233 (short isoform) with His_8 N-terminal fusion. This construct only contains one C-terminal Y residue (Y171). All other Y, including Y132, Y191, and Y226, were mutated to F.
LAT-FFYF	GGSLEHHHHHHHHGIQFKRPHTVAPWPPAFPP VTSFPPLSQPDLLPIPRSPQPLGGSHRTPSSRRDS DGANSVASFENEEPACEDADEDEDDFHNPGFL VVLPDSTPATSTAAPSAPALSTPGIRDSAFSMESI DDFVNVPESGESAEASLDGSREYVNVSQELHP GAAKTEPAALSSQEAEEVEEEGAPDFENLQELN	Human, residues 48-233 (short isoform) with His_8 N-terminal fusion. This construct only contains one C-terminal Y residue (Y191). All other Y, including Y132, Y171, and Y226, were mutated to F.
LAT-FFFY	GGSLEHHHHHHHHGIQFKRPHTVAPWPPAFPP VTSFPPLSQPDLLPIPRSPQPLGGSHRTPSSRRDS DGANSVASFENEEPACEDADEDEDDFHNPGFL VVLPDSTPATSTAAPSAPALSTPGIRDSAFSMESI DDFVNVPESGESAEASLDGSREFVNVSQELHPG AAKTEPAALSSQEAEEVEEEGAPDYENLQELN	Human, residues 48-233 (short isoform) with His_8 N-terminal fusion. This construct only contains one C-terminal Y residue (Y226). All other Y, including Y132, Y171, and

		Y191, were mutated to F.
LAT-FYYY	GGSLEHHHHHHHHGIQFKRPHTVAPWPPAFPP VTSFPPLSQPDLLPIPRSPQPLGGSHRTPSSRRDS DGANSVASFENEEPACEDADEDEDDFHNPGFL VVLPDSTPATSTAAPSAPALSTPGIRDSAFSMESI DDYVNVPESGESAEASLDGSREYVNVSQELHP GAAKTEPAALSSQEAEEVEEEGAPDYENLQEL N	Human, residues 48-233 (short isoform) with His_8 N-terminal fusion. This construct only contains three C-terminal Y residues (Y171, Y191, and Y226). All other Y, including Y132 were mutated to F.
LAT-YFYY	GGSLEHHHHHHHHGIQFKRPHTVAPWPPAFPP VTSFPPLSQPDLLPIPRSPQPLGGSHRTPSSRRDS DGANSVASFENEEPACEDADEDEDDFHNPGYL VVLPDSTPATSTAAPSAPALSTPGIRDSAFSMESI DDFVNVPESGESAEASLDGSREYVNVSQELHP GAAKTEPAALSSQEAEEVEEEGAPDYENLQEL N	Human, residues 48-233 (short isoform) with His_8 N-terminal fusion. This construct only contains three C-terminal Y residues (Y132, Y191, and Y226). All other Y, including Y171 were mutated to F.
LAT-YYFY	GGSLEHHHHHHHHGIQFKRPHTVAPWPPAFPP VTSFPPLSQPDLLPIPRSPQPLGGSHRTPSSRRDS DGANSVASFENEEPACEDADEDEDDFHNPGYL VVLPDSTPATSTAAPSAPALSTPGIRDSAFSMESI DDYVNVPESGESAEASLDGSREFVNVSQELHP GAAKTEPAALSSQEAEEVEEEGAPDYENLQEL N	Human, residues 48-233 (short isoform) with His_8 N-terminal fusion. This construct only contains three C-terminal Y residues (Y132, Y171, and Y226). All other Y, including Y191 were mutated to F.
LAT-YYYF	GGSLEHHHHHHHHGIQFKRPHTVAPWPPAFPP VTSFPPLSQPDLLPIPRSPQPLGGSHRTPSSRRDS DGANSVASFENEEPACEDADEDEDDFHNPGYL VVLPDSTPATSTAAPSAPALSTPGIRDSAFSMESI DDYVNVPESGESAEASLDGSREYVNVSQELHP GAAKTEPAALSSQEAEEVEEEGAPDFENLQELN	Human, residues 48-233 (short isoform) with His_8 N-terminal fusion. This construct only contains three C-terminal Y residues (Y132, Y171, and Y191). All other Y, including Y226 were mutated to F.
Lck	ANSLEPEPWFFKNLSRKDAERQLLAPGNTHGS FLIRESESTAGSFSLSVRDFDQNQGEVVKHYKI RNLDNGGFYISPRITFPGLHDLVRHYTNASDGL CTKLSRPCQTQKPQKPWWEDEWEVPRETLKL VERLGAGQFGEVWMGYYNGHTKVAVKSLKQ GSMSPDAFLAEANLMKQLQHPRLVRLYAVVTQ EPIYIITEYMENGSLVDFLKTPSGIKLNVNKLLD MAAQIAEGMAFIEEQNYIHRDLRAANILVSDTL SCKIADFGLARLIEDNEYTAREGAKFPIKWTAP EAINYGTFTIKSDVWSFGILLTEIVTHGRIPYPG MTNPEVIQNLERGYRMVRPDNCPEELYHLMM LCWKERPEDRPTFDYLRSVLDDFFTATEGQFQP QP	Human, residues 119-509. Y505F mutation prevents autoinhibition to make Lck constitutively active. Lck was used to phosphorylate CD3ζ in solution prior to experimentation on membranes using pCD3ζ.
ZAP70	GPTRMDKDCEMKRTTLDSPLGKLELSGCEQGL HEIKLLGKGTSAADAVEVPAPAAVLGGPEPLMQ ATAWLNAYFHQPEAIEEFPVPALHHPVFQQESF TRQVLWKLLKVVKFGEVISYQQLAALAGNPAA TAAVKTALSGNPVPILIPCHRVVSSSGAVGGYEG GLAVKEWLLAHEGHRLGKPGLGGSGSGSGGG GSSTRMPDPAAHLPFFYGSISRAEAEEHLKLAG MADGLFLLRQCLRSLGGYVLSLVHDVRFHHFI ERQLNGTYAIAGGKAHCGPAELCEFYSRDPDG LPCNLRKPCNRPSGLEPQPGVFDCLRDAMVRD	Human, residues 1 - 619 fused with an N-terminal SNAP tag

	YVRQTWKLEGEALEQAIISQAPQVEKLIATTAH ERMPWYHSSLTREEAERKLYSGAQTDGKFLLR PRKEQGTYALSLIYGKTVYHYLISQDKAGKYCI PEGTKFDTLWQLVEYLKLKADGLIYCLKEACP NSSASNASGAAAPTLPAHPSTLTHPQRRIDTLNS DGYTPEPARITSPDKPRPMPMDTSVYESPYSDP EELKDKKLFLKRDNLLIADIELGCGNFGSVRQG VYRMRKKQIDVAIKVLKQGTEKADTEEMMRE AQIMHQLDNPYIVRLIGVCQAEALMLVMEMA GGGPLHKFLVGKREEIPVSNVAELLHQVSMGM KYLEEKNFVHRDLAARNVLLVNRHYAKISDFG LSKALGADDSYYTARSAGKWPLKWYAPECINF RKFSSRSDVWSYGVTMWEALSYGQKPYKKM KGPEVMAFIEQGKRMEPPECPPELYALMSDCWI YKWEDRPDFLTVEQRMRACYYSLASKVEGPP GSTQKAEAACA	

Table S2. Sequences of constructs used in the study.